



**APPENDIX A
PUBLICATIONS**

ลิขสิทธิ์มหาวิทยาลัยเชียงใหม่

Copyright© by Chiang Mai University
All rights reserved




APPENDIX A.1

Paper in International Journals

ลิขสิทธิ์มหาวิทยาลัยเชียงใหม่

Copyright© by Chiang Mai University
All rights reserved

The seal of Chiang Mai University is a large, light-gray circular emblem in the background. It features an elephant in the center, holding a parasol with a flame on top. The Thai text "มหาวิทยาลัยเชียงใหม่" (Mahavithayalai Chiang Mai) is written in a circle around the elephant. Below the elephant, the English text "CHIANG MAI UNIVERSITY" is visible, along with the year "1964" on the right side.

Nopparat Katkhaw, Nat Vorayos, Tanongkiat Kiatsiroat, Yottana Khunatorn and
Damorn Bunturat, Atipoang Nuntaphan, 2014. Heat Transfer Behavior of Flat Plate
having 45° Ellipsoidal Dimpled Surfaces, *Case Studies in Thermal Engineering*, 2, 67-

74

ลิขสิทธิ์มหาวิทยาลัยเชียงใหม่
Copyright© by Chiang Mai University
All rights reserved



Contents lists available at ScienceDirect

Case Studies in Thermal Engineering

journal homepage: www.elsevier.com/locate/csited

Heat transfer behavior of flat plate having 45° ellipsoidal dimpled surfaces

Nopparat Katkhaw^a, Nat Vorayos^{a,*}, Tanongkiat Kiatsiriroat^a, Yottana Khunatorn^a, Damorn Bunturat^a, Atipoang Nuntaphan^b^a Department of Mechanical Engineering, Chiang Mai University, Chiang Mai 50202, Thailand^b Thermal Technology Research Laboratory, Mae Moh Training Center, Electricity Generating Authority of Thailand, Mae Moh, Lampang 52220, Thailand

ARTICLE INFO

Article history:

Received 25 November 2013

Accepted 22 December 2013

Available online 28 December 2013

Keywords:

Vortex

Dimple

Enhanced heat transfer

ABSTRACT

Flat surface with ellipsoidal dimple of external flow was investigated in this study. 10 types of dimple arrangements and dimple intervals are studied. The stream of air flows over the heated surface with dimples. The velocity of the air stream varies from 1 to 5 m/s. The temperature and velocity of air stream and temperature of dimpled surfaces were measured. The heat transfer of dimpled surfaces was determined and compared with the result of smooth surface. For the staggered arrangement, the results show that the highest heat transfer coefficients for dimpled surfaces are about 15.8% better than smooth surface as dimple pitch of $S_T/D_{minor} = 3.125$ and $S_L/D_{minor} = 1.875$ yield the highest heat transfer coefficient values. And for the inline arrangement, the results show that the heat transfer coefficients for dimples surfaces are about 21.7% better than smooth surface as dimple pitch of $S_T/D_{minor} = 1.875$ and $S_L/D_{minor} = 1.875$ yield the highest heat transfer coefficient values.

© 2014 The Authors. Published by Elsevier Ltd. This is an open access article under the CC BY-NC-ND license (<http://creativecommons.org/licenses/by-nc-nd/3.0/>).

1. Introduction

There are many thermal applications where the fluid-to-gas heat exchanger is a crucial element. The conventional enhanced heat transfer approaches such as fins, baffles, turbulizers etc., always increase either the heat transfer surface area or turbulence or both. These approaches are effective in increasing heat transfer rates; however, this also results in the significant pressure drops. The dimpled surface is a special method for improving the heat transfer rates without the significant pressure drop. Normally, the dimple generates the vortex flow within its hole and the augmentation of heat transfer is obtained [1].

Recently, dimples or concave surfaces have been in focus extensively. In the early investigations, Afansayev et al. [2] investigated the overall heat transfer and pressure drop for turbulent flow flat surface with staggered array of spherical dimples. Significant (30–40%) increases in heat transfer without appreciable pressure losses are reported.

Chyu et al. 1997 [3] studied the heat transfer coefficient distributions of air flow in the channel over flat surface indent with staggered arrays of two different shaped dimple. Their result shows that the local heat transfer coefficients are significantly higher than values in the channels with smooth surfaces. Enhancements are of about 2.5 times of smooth surface values, and pressure losses are about half the values produced by conventional rib turbulators.

Mahmood et al. [4] describe the flow structure above the dimpled flat surface. Flow visualizations showed vortical fluid as vortex pairs shed from the dimples. Their results showed the existence of a low heat transfer region in the upstream half

* Corresponding author. Tel.: +66 53 944146; fax: +66 53 944145.

E-mail addresses: natvorayos@hotmail.com (N. Vorayos), atipoang.n@egat.co.th (A. Nuntaphan).

<http://dx.doi.org/10.1016/j.csite.2013.12.002>

2214-157X © 2014 The Authors. Published by Elsevier Ltd. This is an open access article under the CC BY-NC-ND license (<http://creativecommons.org/licenses/by-nc-nd/3.0/>).

Nomenclature		h	Average heat transfer coefficient (W/m ² K)
A	Area (m ²)	h_0	Average heat transfer coefficient of flat plate without dimple (W/m ² K)
D	Dimple diameter (mm)	h_x	Local heat transfer coefficient (W/m ² K)
D_{minor}	Dimple diameter on minor axis (mm)	S_L	Streamwise pitch (mm)
Nu	Average Nusselt number	S_T	Spanwise pitch (mm)
Nu_x	Local Nusselt number	T	Temperature (°C)
Nu_0	Baseline average Nusselt number of flat plate without dimple	V	Velocity (m/s)
Pr	Prandtl number	x	Spanwise coordinate
Re_x	Reynolds number base surface length (include dimples surface)	y	Streamwise coordinate

of the dimple cavity followed by a high heat transfer region in the downstream half. Additional regions of high heat transfer were identified at the downstream rim of the dimple and on the flat surface downstream of each dimple.

Ligrani et al. [5] reported that as the H/D (channel height to dimple diameter) increases the secondary flow structures and flow mixing intensified decreased. Nevertheless, Moon et al. [6] obtained almost a constant heat augmentation ratio of 2.1 for a dimpled passage with H/D from 0.37 to 1.49.

Burgess et al. [7] reported that both the Nusselt number and the friction augmentation increased as the dimple depth increased. These are attributed to (i) increases in the strengths and intensity of vortices and associated secondary flows ejected from the dimples, as well as (ii) increases in the magnitudes of three-dimensional turbulence production and turbulence transport. The effects of these phenomena are especially apparent in the local Nusselt number just inside, and on the downstream edges of the dimples.

Wang et al. [8] investigated a novel enhanced heat transfer tube with ellipsoidal dimples. Their computed results indicated that the Nusselt number for ellipsoidal dimpled tube and spherical dimpled tube are 38.6–175.1% and 34.1–158% higher than that for the smooth tube, respectively. The friction factors of dimpled tube increase by 26.9–75% and 32.9–92% for ellipsoidal and spherical dimples compared with the smooth tube respectively.

Katkhaw et al. [9] studied the heat transfer of air flow over dimpled flat surface with the 14 types of dimpled arrangement. Their results show that heat transfer coefficients for dimpled surfaces are about 26% better than smooth surface for staggered arrangement. And for the inline arrangement, the results show that heat transfer coefficients for dimples surfaces are about 25% better than smooth surface.

This study proposes to employ the ellipsoidal dimple on the flat surface to observe the thermal characteristic of air flow. In addition, the effect of dimple arrangements, and dimple pitch will be included in this work. The results of this research aim to serve the heat exchanger application.

2. Experimental setup and procedure

The schematic diagram of the experimental setup for heat transfer measurements is shown in Fig. 1. The fluid used in the apparatus is air at room temperature, which is generated by an air blower. The stream of air flows through the test section and flows over test surface. In this experiment, the velocity of air stream was controlled by the frequency inverter with the controllable range of 1–5 m/s. The velocity of air stream was measured by a hot wire anemometer with ± 0.2 m/s accuracy. The surface temperature of flat plate was measured by infrared imaging camera with ± 2 °C accuracy, where the measuring instrument was also calibrated to surface temperature with T-type thermocouple. The inlet temperature of air stream was measured by a T-type thermocouple with ± 0.1 °C accuracy.

The test kit comprises test plate and plate heater. Test plates are made from 1.5 mm thickness acrylic which is depressed in any configurations of dimple. The iron powder was filled beneath the tested plate to avoid the space between the plate and electric heater. The exterior of the test kit was insulated with three layers of 2.5 cm-thickness glass wool insulation to minimize heat loss. The electric heater supplies a constant heat flux, where the power to the heater was controlled and regulated by a variac power supply. T-type thermocouples are located between each layer to determine conduction losses.

Figs. 2 and 3 illustrate the geometric details of the tested surface indent with arrays of ellipsoidal dimple. Dimples were employed in an inline and staggered array. Table 1 lists the details of the test case.

3. Data reduction

During the experiment, inlet air stream velocity, temperature, the tested surface temperature and power supply were measured to determine the local heat transfer coefficient (h_x), which is calculated from

$$h_x = q_s' / (T_s - T_\infty) \quad (1)$$

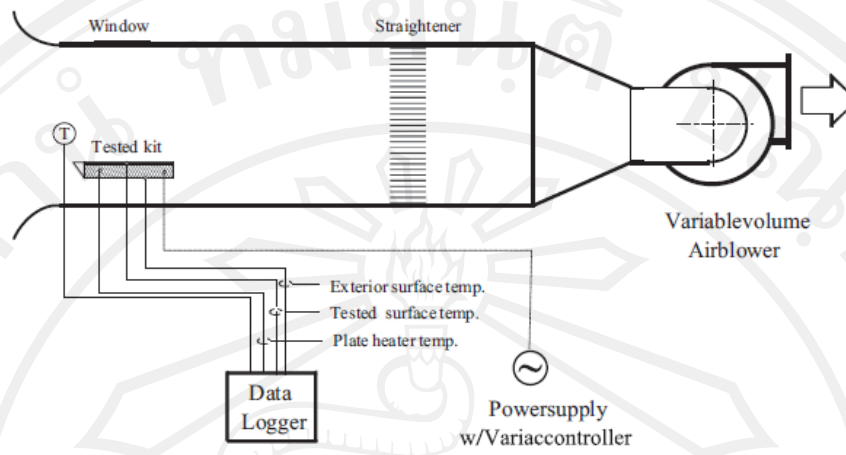


Fig. 1. Schematic diagram of the experimental setup.

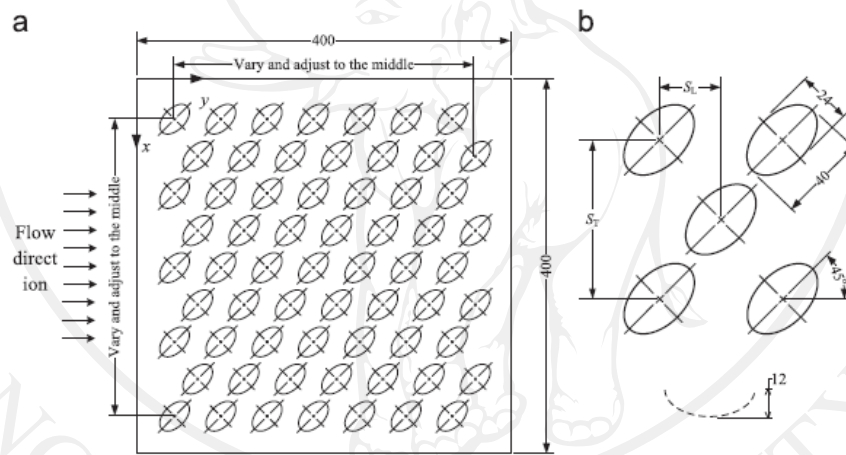


Fig. 2. Details of (a) dimpled-tested surface for staggered arrangement and (b) individual dimple geometry. All dimensions are in mm.

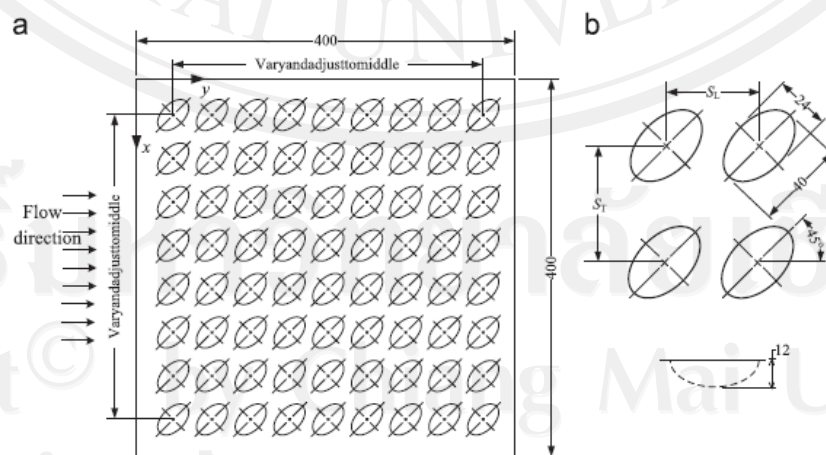


Fig. 3. Details of (a) dimpled-tested surface for inline arrangement and (b) individual dimple geometry. All dimensions are in mm.

Table 1
Geometric dimensions of dimpled surface.

No	S_T (mm)	S_L (mm)	Arrangement	S_T/S_L
1	50	40	Staggered	1.25
2	50	45	Staggered	1.11
3	50	50	Staggered	1.00
4	60	45	Staggered	1.33
5	75	45	Staggered	1.67
6	40	40	Inline	1.00
7	40	45	Inline	1.89
8	40	50	Inline	0.80
9	45	45	Inline	1.00
10	50	45	Inline	1.11

where q_s' is surface heat flux which is calculated from heat rate level at the tested surface and is divided by the total tested surface area (flat portions and dimpled surface). T_s is the local surface temperature and T_a is the temperature of inlet air stream flowing over the tested plate.

The averaged air side heat transfer coefficient (h) of the tested surface is determined by integrating all of the area of tested surface as

$$h = \frac{1}{A_s} \int_{A_s} q_s' / (T_s - T_\infty) dA_s \quad (2)$$

where A_s is the tested surface area comprising of flat portions and dimpled surfaces.

The averaged Nusselt number (Nu_L) is defined as

$$Nu_L = \frac{hL}{k_f} \quad (3)$$

where L is maxima stream-wise surface length comprising of flat portions and dimple portions. k_f is the thermal conductivity of air stream.

Reynolds number (Re_L) for air flow is defined as

$$Re_L = \frac{\rho_f V_f L}{\mu_f} \quad (4)$$

where ρ_f , V_f and μ_f are the density of air, the air frontal velocity and the dynamic viscosity of air stream, respectively.

This experiment is a further study from Katkhaw et al. [9]. The previous and current results will be in comparison with existing correlation of the heat transfer of parallel flow over flat plate with constant heat flux [10] under the lamina flow condition.

4. Results and discussion

4.1. Staggered arrangement

There are five samples in the case of staggered arrangement as shown in Table 1. For Geometries nos. 1–3, S_T is constant and S_L varies. For Geometries nos. 2, 4, and 5, S_L is constant and S_T varies. Fig. 4 shows the temperature distribution along the dimpled surface, which is captured by the infrared imaging camera. At frontal velocity of 2.9 m/s for Geometry No. 1, flow direction for the figure is from the left to right. As shown in the figure, the location of ellipsoidal dimples conforms to the ellipsoidal temperature contour. Whole area of plain surface is at lower temperature than dimple area. Higher temperature is located at the upstream half and gradually increases along the downstream half. The lowest temperature occurs in the downstream rim of the dimples and obviously decreases downstream on plain surfaces. In case of spherical dimples, Mahmood et al. [6] pointed out that this is due to air stream flowing over the spherical dimples, and then shedding fluid and vortex pairs shed from the dimple.

Fig. 5 shows the effect of S_T and S_L on the air side heat transfer performance. Results are termed as heat transfer coefficient vs. frontal velocity. As shown in the figure, the total heat transfer coefficient is rather constant while S_L increases because the dimple indent establishes the weak heat transfer area inside the dimple and enhances the heat transfer area outside the dimple, and the enhanced area is kept close to the dimple. From Geometry Nos. 1–3, as S_T remains constant, heat transfer characteristic is not varied in spite of the fact that S_L differs within 20%. This suggests the independence of heat convection characteristic from S_L . However, this may be because the number of dimples is also decreased by 22%.

Similarly, for Geometry Nos. 2, 4 and 5, as S_T varies by 30%, heat transfer characteristic does not change significantly, but it increases distinctively by 15.8% when S_T is 75 mm. (50% from Geometry No. 2).

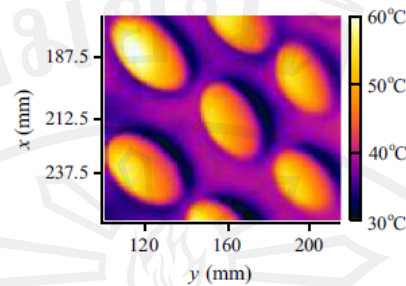


Fig. 4. Temperature distributions of Geometry No. 1 at frontal velocity = 2.9 m/s.

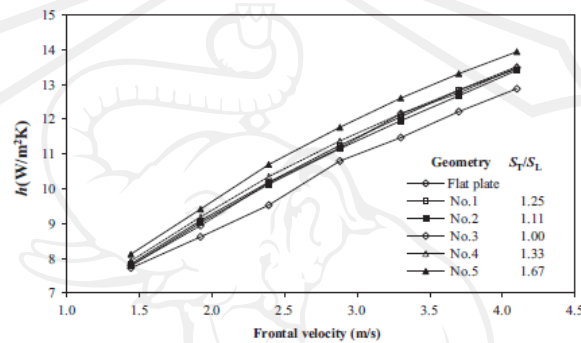


Fig. 5. Effect of dimple arrangement on heat transfer coefficient for staggered arrangement.

Fig. 6 shows the heat transfer coefficient of this study in comparison with that of spherical dimple surface [9]. The result shows that, for staggered arrangement, the spherical dimple surface significantly yields the higher heat transfer coefficient than ellipsoidal dimple surface.

4.2. Inline arrangement

In the case of inline arrangement, there are five categories shown in Table 1. For Geometry Nos. 6–8, S_T is constant and S_L is varied. While for Geometry Nos. 7, 9, and 10, S_L is constant and S_T is varied. In Fig. 7, the temperature distribution along the tested surface is shown, with an air flow direction from left to right. As in the figure, it shows that the temperature distribution inside and around the dimples is similar to staggered arrangement. The temperature distribution is higher in the upstream halves of the dimples and decreases progressively downstream of the dimples, which then becomes lowest near the downstream edges.

Fig. 8 shows the effect of dimple arrangement on heat transfer coefficient. As shown in the figure, Geometry No. 6 shows lower heat transfer coefficient in the lower flat plate. As the temperature of the inner side of dimple is low, too many dimples cause less heat transfer. As S_L increases heat transfer coefficient slightly increases. This is possibly due to the enhanced heat transfer area increasing. Similarly, heat transfer coefficient increases while S_T increases from 40 mm to 45 mm because of the increasing of enhanced heat transfer area. However, heat transfer coefficient decreases while S_T increases beyond 45 mm, but less than 50 mm. This finding is similar to staggered arrangement. From the figure, Geometry No. 9 yields the highest heat transfer coefficient of about 21.7% better than the flat plate and Geometry No. 6 yields the lowest heat transfer coefficient.

Fig. 9 shows the comparison of the heat transfer coefficients of the ellipsoidal dimple surface of this study to those of spherical dimple surface [9]. The result shows that, for inline arrangement, the spherical dimple surface yields lower heat transfer coefficients than those of ellipsoidal dimple surface significantly.

4.3. Empirical correlation

Based on the previous results, the test data of inline and staggered arrangements yield complex behavior. The corresponding correlations are reported separately by inline and staggered configuration. The multiple linear regression technique is performed to obtain the relevant correlations. The corresponding correlations are obtained as follows:

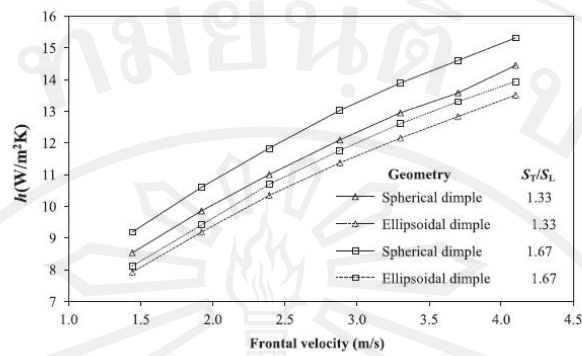


Fig. 6. Comparison of heat transfer coefficient for staggered arrangement of spherical dimple surface and the ellipsoidal dimple surface.

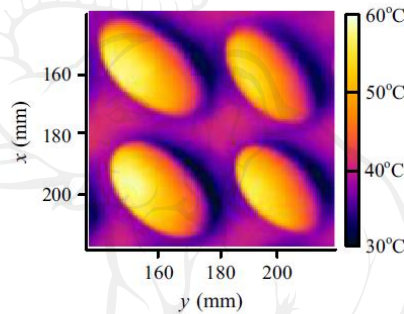


Fig. 7. Temperature distributions of Geometry No. 6 at frontal velocity is 4.1 m/s.

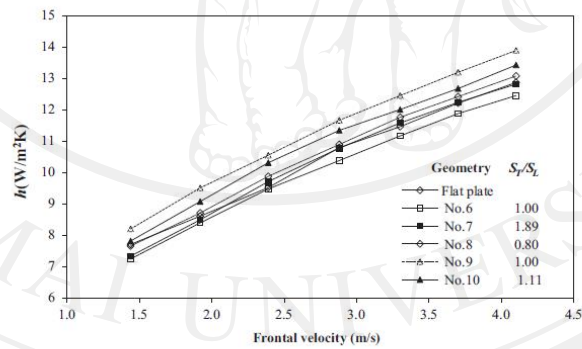


Fig. 8. Effect of dimple arrangement on heat transfer coefficient for inline arrangement.

Correlation of the Nusselt numbers for the staggered arrangement:

$$\frac{Nu}{Nu_0} = 1.1067 \left(\frac{S_T}{S_L} \right)^{0.0992} \quad (5)$$

Correlation of the Nusselt numbers for the inline arrangement:

$$\frac{Nu}{Nu_0} = 0.904 \left(\frac{S_L}{S_T} \right)^{0.0944} \left(\frac{S_T}{D} \right)^{0.3995} \quad (6)$$

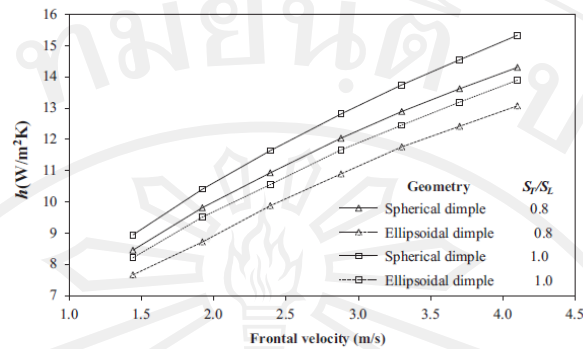


Fig. 9. Comparison of heat transfer coefficient for staggered arrangement of spherical dimple surface and the ellipsoidal dimple surface.

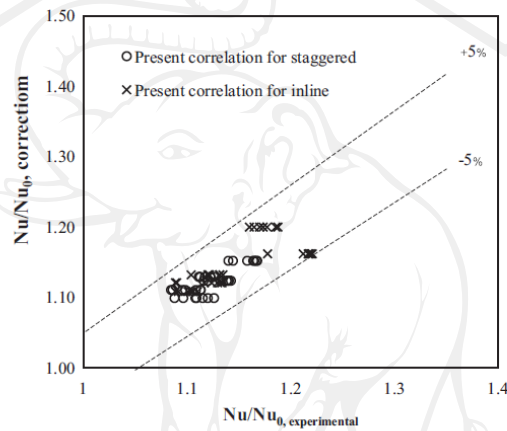


Fig. 10. Comparison of heat transfer correlations with experimental data.

The comparison of the experimental results with the proposed correlations is showed in Fig. 10. The aforementioned can predict 97% and 95% of the experimental data, with $\pm 5\%$. The standard deviation of the correlations Eqs. (5) and (6) are 1.3% and 2.54% respectively.

4.4. Discussion

From the literature, Wang et al. [8] report that the Nusselt number of flow inside tube with ellipsoidal dimples are higher than the tube with spherical dimples. Nevertheless, the Nusselt number for external air flow over flat surface with dimples has not been reported. Katkhaw et al. [9] report that the maximum enhanced heat transfer is about 25.8% for flat surface with spherical dimples. From this work, the maximum enhanced heat transfer of 21.7% from ellipsoidal dimple is reported in comparison with that of flat surface. Moreover the enhancement depends on configuration.

5. Conclusion

The present work reports the heat transfer performance of external air flow over the ellipsoidal dimple surface. The dimple arrangement and dimple interval are examined. Based on the previous result and discussions, these conclusions are obtained:

1. The air side heat transfer performance is augmented approximately 10–22% at all Reynolds Numbers and all dimple arrangements.
2. For staggered arrangements, the dimples pitch of $S_L/D_{\text{minor}}=1.875$ and $S_T/D_{\text{minor}}=1.875$ yields the optimum thermal resistance values of about 21.7% better than flat plate.
3. For inline arrangements, the dimples pitch of $S_L/D_{\text{minor}}=1.875$ and $S_T/D_{\text{minor}}=3.125$ yields the optimum thermal resistance values of about 15.8% better than flat plate.

4. Correlations of the present experiment in both staggered and inline arrangement are obtained and the proposed correlations yield fairly good predictive ability against the present test data.

Acknowledgments

The authors would like to thank the Thermal Technology Research Laboratory at the Mae Moh Training Center Electricity Generating Authority of Thailand for facilitating the testing equipment and the Department of Mechanical Engineering, Faculty, Chiang Mai University for funding this research study.

References

- [1] Chudnovsky Y, A Kozlov. Development and field trial of dimpled-tube technology for chemical Industry process heaters, Final report, Industrial Technology Program, U.S. Department of Energy; September 2006.
- [2] Afanasyev VN, Chudnovsky YP, Leontiev AI, Roganov PS. Turbulent flow friction and heat transfer characteristics for spherical cavities on a flat plate. *Exp Therm Fluid Sci* 1993;7(1):1–8.
- [3] Chyu MK, Yu Y, Ding H, Downs JP, Soechting FO. Concavity enhanced heat transfer in an internal cooling passage. ASME Paper 97-GT-437; 1997.
- [4] Mahmood GI, Hill ML, Nelson DL, Ligrani PM, Moon HK, Glezer B. Local heat transfer and flow structure on and above a dimpled surface in a channel. *J Turbomach* 2001;123(1):115–23.
- [5] Ligrani PM, Harrison JL, Mahmood GI, Hill ML. Flow structure due to dimple depressions on a channel surface. *Phys Fluids* 2001;13(11):3442–51.
- [6] Moon HK, O'Connell T, Glezer B. Channel height effect on heat transfer and friction in a dimpled passage. *J Eng Gas Turbines Power* 2000;122(2):307–13.
- [7] Burgess NK, Ligrani PM. Effects of dimple depth on channel Nusselt numbers and friction factors. *J Heat Transfer* 2005;127(1):839–47.
- [8] Wang Y, He YL, Lei YG, Zhang J. Heat transfer and hydrodynamics analysis of a novel dimpled tube. *Exp Therm Fluid Sci* 2010;34(8):1273–81.
- [9] Katkhaw N, Vorayos N, Kiatsiriroat T, Khunatom Y, Bunturat D, Nuntaphan A. Heat transfer behavior of flat plate having spherical dimpled surfaces. *Int Commun Heat Mass Transfer* 2014 (submitted for publication).
- [10] Incropera FP, Dewitt DP, Bergman TL, Lavine AL. *Introduction to Heat Transfer*. 5th ed. Asia: John Wiley & Sons; 2007.



APPENDIX A.2
Paper in Conferences

ลิขสิทธิ์มหาวิทยาลัยเชียงใหม่

Copyright© by Chiang Mai University
All rights reserved



Nopparat Katkhaw, Nat Vorayos, Atipoang Nuntaphan, 2014. Heat Transfer Behavior of Flat Plate having Dimple Surfaces, โครงการจัดประชุมวิชาการ การถ่ายทอดผลงาน ความร้อน และมวลในอุปกรณ์ด้านความร้อนและกระบวนการ ครั้งที่ 13, เจ้าหลวงคานานารีรีสอร์ท อำเภอท่าใหม่ จังหวัดจันทบุรี, มีนาคม 2557, หน้า 391-396

ลิขสิทธิ์มหาวิทยาลัยเชียงใหม่
Copyright© by Chiang Mai University
All rights reserved



การถ่ายทอด พลังงานความร้อนและมวล

ในอุปกรณ์ด้านความร้อนและกระบวนการ ครั้งที่ 13

วันที่ 13-14 มีนาคม 2557

ณ เจ้าหลาว คาบาน่า รีสอร์ท จังหวัดจันทบุรี



Heat Transfer Behavior of Flat Plate having Dimple Surfaces

Nopparat Katkhaw¹

Nat Vorayos¹

Atipoang Nuntaphan²

¹Department of Mechanical Engineering
Faculty of Engineering, Chiang Mai
University

Chiang Mai, Thailand, 50200.

Tel. 053-944146, Fax. 053-944145

Email: nopparat_ka@hotmail.com

Email: natvorayos@hotmail.com

²Thermal Technology Research Laboratory,

Mae Moh Training Center,

Mae Moh, Lampang 52220

Electricity Generating Authority of Thailand

Abstract In the present study, heat transfer analysis of dimpled surfaces of external flow was investigated. The effect of dimpled geometries, the dimple depth, and the attack angle of the ellipsoidal dimple was simulated. The SOLIDWORKS Flow Simulation 2012 is employed for all numerical predictions. The simulations were carried out with air stream flows over the isothermal dimple surface. The entrance air velocity is varied from 1 to 4 m/s. The heat transfer performance and surface friction coefficient of dimple surfaces were investigated and compared with the result of smooth surface. As the result, the ellipsoidal dimple surface with depth of $0.2D_{major}$ and 45° attack angle is the best configuration which gives the highest effectiveness.

Keyword Vortex, Dimple, Enhanced Heat transfer

1. Introduction

There are many thermal applications where the fluid-to-gas heat exchanger is crucial element. The conventional enhanced heat transfer approaches such as fins, baffles, turbulizers and etc., always increase either the heat transfer surface area or turbulence or both. These approaches are effective in increasing heat transfer rates; however, this also results to the significant pressure drops. The dimple surface is a special method for improving the heat transfer rates without the significant pressure drop. Normally, the dimple generates the vortex flow within its hole and the augmentation of heat transfer is obtained [1] as illustrated in Figure 1, each dimple works as a vortex generator that intensifies the rate of convective heat transfer and mass transfer to the dimpled surfaces

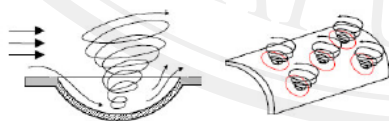


Figure 1 Vortex generation on dimple surfaces (From Chudnovsky and Kozlov [1])

In the early investigations, Afansayev et al. [2] investigated the overall heat transfer rate and the pressure drop for a flat plate having shallow dimples under the turbulent flow of air stream. They found 30-40% increasing of heat transfer

performance with negligible pressure drop. Chyu et al. [3] presented the influences of the concavities imprinted on the surface in the staggered arrays. They found the augmentation of heat transfer rate around 2.5 times compared to the smooth surface. Mahmood et al. [4] studied the flow structure above the dimpled surface by using flow visualization technique and numerical analysis. Their results showed the periodic and the continuous shedding of primary vortex pair from the central portion of the dimple and the secondary vortex pair shed from the span-wise edges of the dimple. Moreover, they found the heat transfer distribution and local Nusselt number variation on the dimpled surface. Their results showed the lower heat transfer region on the upstream half of the dimple cavity followed by the higher heat transfer region on the downstream half. The additional regions of high heat transfer were identified at the downstream rim of the dimple. Ligrani et al. [5] also studied the flow structure of the dimpled channel and the effect of channel height on the vortex form. They found that as the ratio of channel height to dimple print diameter decreases, the strength of the primary vortex pair increases, and two additional secondary vortex pairs which form near the span-wise edges of each dimple become significantly stronger. Ligrani et al. [6] investigated the Nusselt numbers and flow structure on and above a shallow dimpled surface within a channel including the effects of inlet turbulence intensity level. They found that the highest local Nusselt number ratios are presented within the

downstream portions of dimples, as well as near dimple span-wise and downstream edges. Local and spatially averaged Nusselt number ratios sometimes change by small amounts as the channel inlet turbulence intensity level is altered, whereas friction factor ratios increase somewhat at the channel inlet turbulence intensity level increases. Burgess et al. [7] studied the effect of dimple depth on the Nusselt number and they reported that both the Nusselt number and the friction augmentation increased with the raising of dimple depth.

From the literatures, their results show the superior performance of dimple surface. However, the influence of some dimple geometry on the heat transfer performance has not report. Therefore, the objective of this study is to observe the thermal characteristic of air flow over flat plate having dimpled surface. In addition, the effect of dimpled geometries (spherical and ellipsoidal shape), the dimple depth, and the attack angle of the ellipsoidal dimple will be included in this work by numerical simulation. The results of this research aim to serve the heat exchanger application.

2. Problem definition

2.1 Problem conditions and main assumptions

Figure 2 shows the test surface which single dimple indent is employed. The problem under consideration is an external air flow over the isothermal plate and has the following conditions.

- The fluid is air at 300 K.
- The entrance air velocity is varied from 1 to 4 m/s.
- A constant surface temperature of 400 K is applied to the dimple and plan surface.
- Inlet turbulent intensity level (TI) of 3% is used.
- The air flow is assumed to be steady state in three-dimensional domain.

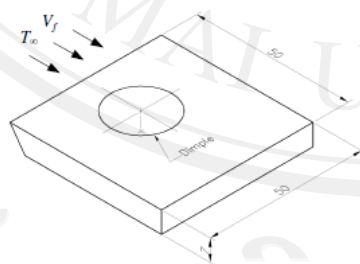


Figure 2 Details dimple geometry (all dimensions are in mm).

2.2 Numerical method

The numerical solutions of mixed convection of laminar and turbulent are obtained by using the SOLIDWORKS Flow Simulation 2012. The $k-\varepsilon$ model [8] is employed as the

turbulence model for all numerical predictions.

Figure 3 shows a side view of the computational grid which is employed for dimple surfaces.

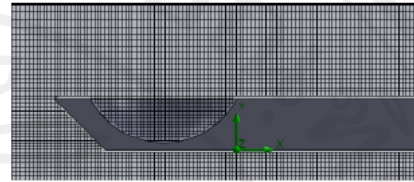


Figure 3 computational grids for dimple surfaces.

3. Results and discussions

3.1 Data reduction

After simulation is finish, the surface heat transfer rate and surface friction force are obtained to determine the heat transfer coefficient and surface friction coefficient. The averaged air side heat transfer coefficient (h) is calculated by

$$h = q'' / (T_s - T_\infty) \quad (1)$$

where q'' is surface heat flux. The heat flux is calculated from heat rate level at the tested surface under the total surface area (flat portion and dimple surface). T_s is surface temperature and T_∞ is temperature of inlet air stream flowing over the tested plate.

The average surface friction coefficient is calculated by

$$C_f = \frac{F_{s,x}}{\rho V_f^2 A / 2} \quad (2)$$

where $F_{s,x}$ is surface friction force in x-direction. ρ and V_f are the density of air and air frontal velocity respectively. A is the total surface area (flat portion and dimple surface).

For comparing the integrated performance of dimple surface, the effectiveness (E) factor is obtained as the performance criterion. It is defined as the heat transfer ratio under the friction coefficient ratio.

$$E = (h/h_0) / (C_f/C_{f,0}) \quad (4)$$

where h_0 is averaged air side heat transfer coefficient of flat plate, and $C_{f,0}$ is the average surface friction coefficient of flat plate.

Reynolds number (Re_L) for air flow is defined as

$$Re_L = \frac{\rho_f V_f L}{\mu_f} \quad (3)$$

where μ_f is the density of air, the air frontal velocity and the dynamic viscosity of air stream respectively. L is stream-wise surface length.

3.2 Result of base case

The heat transfer and pressure loss of external air flow over the isothermal flat plate without dimple was simulated.

These results are the base case for comparing with dimple surface. The simulated result is shown in figure 4.

From the figure 4, the average heat transfer coefficient values increase as frontal velocity increase. Contrary, the average surface friction coefficient values decrease as frontal velocity increase. It should be notice that the heat transfer coefficient data from the simulation agrees very well with the model [9]. In part of friction coefficient, although the result has error about 10% from the model, it has the same trend with the model.

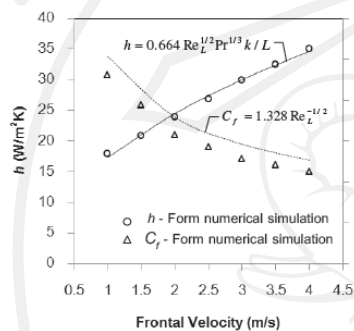


Figure 4 Comparison of the heat transfer coefficient and friction coefficient from the numerical simulation and the model.

3.3 Flow behavior

Figure 5 shows the flow trajectory of spherical dimple surface for frontal velocity of 1 m/s. As shown in the figure, air flow along the plain surface and then, the air flow is induced into the dimple. The recirculating flow is occurred inside the dimple is evident and eject along the downstream line.

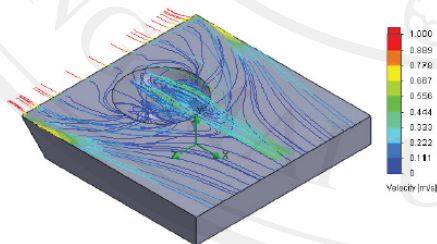


Figure 5 flow trajectory of spherical dimpled surface.

3.4 Effect of dimple shape

In this part, there are three dimple configurations, spherical dimple, and two shapes of ellipsoidal dimple with 45° attack angle as shown in figure 6.

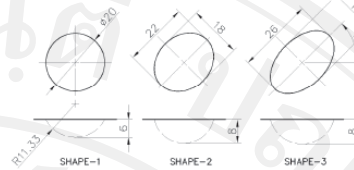


Figure 6 dimple configurations.

Figure 7 shows the effect of dimple shape of the air side heat transfer performance. As shown in the figure, the h/h_0 values are less than 1.0 because in this study, the performance is evaluated only single dimple, which Katkhaw et al. [10] explained that the heat transfer performance will be gradually adopted and increased at the next dimple along the streamline. From the simulated results, the turbulence intensity level increases from SHAPE-1 to SHAPE-3, but SHAPE-1 yields the highest heat transfer coefficient because the total surface area of SHAPE-1 is lower than SHAPE-2 and SHAPE-3 (as Eq.1, h is inverse to surface area). This result is similar to the results of Katkhaw et al. [11].

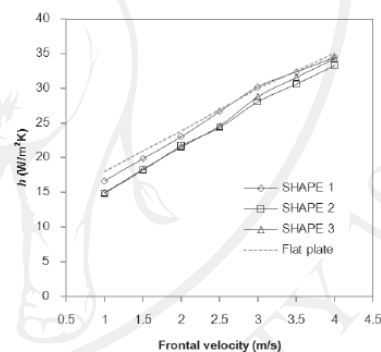


Figure 7 Effect of dimple shape to the air side heat transfer performance.

The effect of dimple shape to the surface friction coefficient is illustrated in figure 8. As shown in the figure, SHAPE-1 has the highest friction coefficient and the SHAPE-2 and SHAPE-3 have the closer values of friction coefficient similar to the results of heat transfer performance.

Figure 9 shows the effect of dimple shape to the effectiveness (E). As shown in the figure, the SHAPE-3 gives higher effectiveness than other shapes at all frontal velocity.

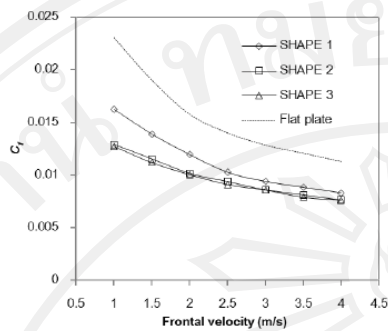
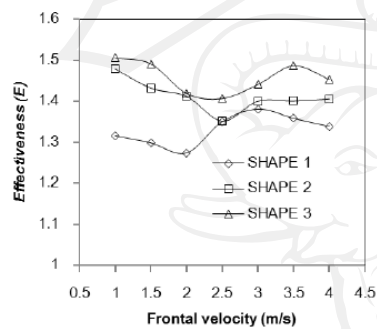
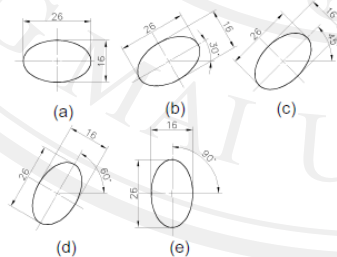


Figure 8 Effect of dimple shape to the surface friction coefficient.

Figure 9 Effect of dimple shape to the effectiveness (E).

3.5 Effect of attack angle of dimple

In this part, the effect of the attack angle of 0° , 30° , 45° , 60° , and 90° of ellipsoidal dimple surface is studied. Figure 10 shows the configuration of ellipsoidal dimples in the various attack angles. The air flow direction is from bottom to top of the figure

Figure 10 Details of: (a) 0° attack angle (b) 35° attack angle (c) 45° attack angle (d) 60° attack angle (e) 90° attack angle.

The effect of attack angle on the air side heat transfer performance is shown in figure 11. It is found that; the heat transfer coefficient values decrease as the attack angles increase because the small attack angles have a larger frontal area than high attack angles.

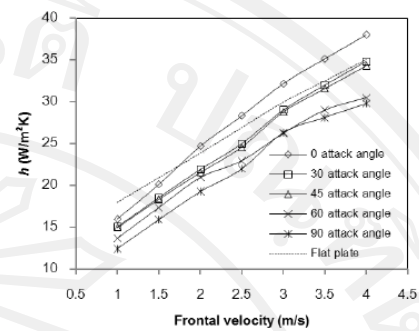


Figure 11 Effect of attack angle on the air side heat transfer performance.

Figure 12 shows the effect of attack angle on the surface friction coefficient. As shown in the figure, the surface friction coefficient values decrease as the attack angles increase similar to the result of heat transfer performance while the 90° attack angle has the considerably higher than other attack angles.

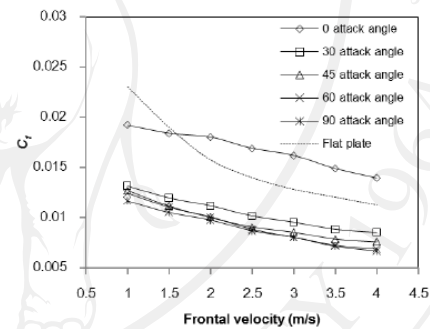
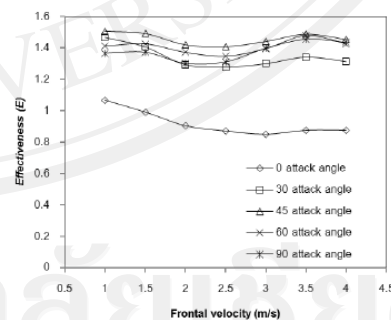


Figure 12 Effect of attack angle on the surface friction coefficient.

Figure 13 Effect of attack angles to the effectiveness (E).

The effectiveness (E) of each attack angles is illustrated in the figure 13. As shown in the figure, the attack

angles of 0° has the extremely low effectiveness and 45° has the slightly effectiveness higher than other attack angles.

3.6 Effect of dimple depth

The depths of $0.1D_{\text{major}}$, $0.2D_{\text{major}}$ and $0.3D_{\text{major}}$ of dimple are shown in the figure 14. The effect of dimple depth to heat transfer performance and surface friction coefficient is studied in this part.

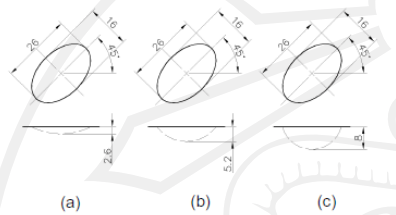


Figure 14 Detail of: (a) $0.1D_{\text{major}}$ of dimple depth (b) $0.2D_{\text{major}}$ of dimple depth (c) $0.3D_{\text{major}}$ of dimple depth.

Figure 15 shows the effect of dimple depth to the air side heat transfer performance. From the simulated results, the turbulence intensity level increases as the depth of dimple increases, but highest heat transfer coefficient decreases as the depth of dimple increases because the total surface area has more influence, which this result is similar to dimple shape condition.

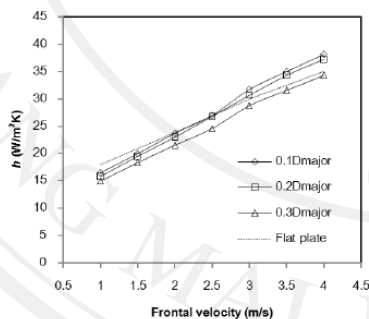


Figure 15 Effect of dimple depth to the air side heat transfer performance.

Figure 16 shows the effect of dimple depth on the surface friction coefficient as a function of frontal velocity. As the results, the surface friction coefficient values decrease as the depths of dimple increase, which this result is similar to the heat transfer performance.

The effectiveness (E) of each dimple depth is shown in figure 17. The dimple depth of $0.2D_{\text{major}}$ has the highest effectiveness.

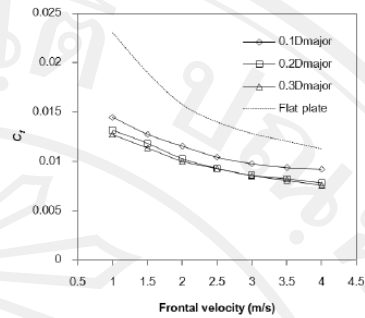


Figure 16 Effect of dimple depth to the surface friction coefficient.

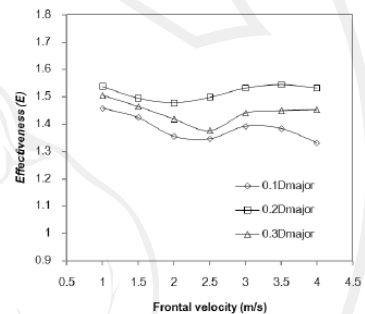


Figure 17 Effect of dimple depth to the effectiveness (E).

4. Summary and conclusion

The present study reports the heat transfer performance of air flow over the dimples surface. The effects of dimples shape, dimple attack angle and dimple depth are examined. On the basis of previous discussions, the conclusions are made:

1. From simulated results, the air flows over the dimple surface is induced into the dimple. The recirculating flow is occurred inside the dimple and eject along the downstream line.
2. Spherical dimple surface gives the higher heat transfer performance than the ellipsoidal dimple. Nevertheless, ellipsoidal dimple surface gives the higher effectiveness (E) than the ellipsoidal dimple.
3. Both heat transfer performance and surface friction coefficient decrease as the attack angles increase while dimple with 45° attack angle gives the highest effectiveness (E).
4. Both heat transfer performance and surface friction coefficient decrease as the depths of dimple increase. The $0.2D_{\text{major}}$ dimple depth yields the highest effectiveness (E).
5. Ellipsoidal dimple surface with $0.2D_{\text{major}}$ and 45° attack angles is the best configuration which gives the highest effectiveness.

Acknowledgement

The authors would like to thank the Thermal Technology Research Laboratory at the Mae Moh Training Center, Electricity Generating Authority of Thailand for facilitating the testing equipment and the Department of Mechanical Engineering, Faculty of Engineering, Chiang Mai University for funding this research study.


Reference

- [1] Y. Chudnovsky, A. Kozlov, Development and field trial of dimpled-tube technology for chemical Industry process heaters, Final report, Industrial Technology Program, U.S. Department of Energy, September 2006.
- [2] V.N. Afanasyev, Y.P. Chudnovsky, A.I. Leontiev, P.S. Roganov, Turbulent flow friction and heat transfer characteristics for spherical cavities on a flat plate. *Experimental Thermal and Fluid Science* 7 (1) (1993) 1-8.
- [3] M.K. Chyu, Y. Yu, H. Ding, J.P. Downs, F.O. Soechting, Concavity enhanced heat transfer in an internal cooling passage, ASME Paper 97-GT-437, 1997.
- [4] G.I. Mahmood, M.L. Hill, D.L. Nelson, P.M. Ligrani, H.K. Moon, B. Glezer, Local heat transfer and flow structure on and above a dimpled surface in a channel, *Journal of Turbomachinery* 123 (1) (2001) 115-123.
- [5] P.M. Ligrani, J.L. Harrison, G.I. Mahmood, M.L. Hill, Flow structure due to dimple depressions on a channel surface, *Physics of Fluids* 13 (11) (2001) 3442-3451.
- [6] P.M. Ligrani, N.K. Burgess, S.Y. Won, Nusselt numbers and flow structure on and Above a shallow dimpled surface within a channel including effects of inlet turbulence intensity level, *ASME Transactions-Journal of Turbomachinery* 127 (2) (2005) 321-330.
- [7] N.K. Burgess, P.M. Ligrani, Effects of dimple depth on channel Nusselt numbers and friction factors, *Journal of Heat Transfer* 127 (1) (2005) 839-847.
- [8] B.E. Launder, D.B. Spalding, *Computer Methods in Applied Mechanics and Engineering*, Computer Methods in Applied Mechanics and Engineering, 3 (2) (1974) 269-289.
- [9] F.P. Incropera, D.P. Dewitt, T.L. Bergman, A.L. Lavine, *Introduction to Heat Transfer*, 5th ed., John Wiley & Sons, Asia, 2007.
- [10] N. Katkhaw, N. Vorayos, T. Kiatsiriroat, Y. Khunatorn, D. Bunturat, A. Nuntaphan, Heat transfer behavior of flat plate having spherical dimpled surfaces, *Journal of Mechanical Science and Technology*, Submitted.
- [11] N. Katkhaw, N. Vorayos, T. Kiatsiriroat, Y. Khunatorn, D. Bunturat, A. Nuntaphan, Heat transfer behavior of flat plate having 45° ellipsoidal dimpled surfaces, *Case Studies in Thermal Engineering*, Accepted.

Nomenclature

A	Area (m^2)
D	Dimple diameter (mm)
D_{minor}	Dimple diameter on minor axis (mm)
D_{major}	Dimple diameter on major axis (mm)
Pr	Prandtl number
Re_L	Reynolds number base surface length
h	Average heat transfer coefficient ($\text{W/m}^2\text{K}$)
h_0	Average heat transfer coefficient of flat plate without dimple ($\text{W/m}^2\text{K}$)
h_x	Local heat transfer coefficient ($\text{W/m}^2\text{K}$)
T	Temperature ($^{\circ}\text{C}$)
V	Velocity (m/s)
x	Spanwise coordinate
y	Streamwise coordinate



The seal of Chiang Mai University is a large, light gray circular emblem in the background. It features an elephant in the center, holding a torch aloft in its trunk. The Thai text "มหาวิทยาลัย เชียงใหม่" is written in a circle around the elephant, and "CHIANG MAI UNIVERSITY 1964" is written in English at the bottom.

Nopparat Katkhaw, Nat Vorayos, Atipoang Nuntaphan, 2014. Thermal Characteristics of Air Flow over Flat Tube with Ellipsoidal Dimpled Surface, โครงการจัดประชุมวิชาการ การถ่ายทอดผลงาน ความร้อน และมวลในอุปกรณ์ด้านความร้อนและกระบวนการ ครั้งที่ 13, เจ้า หลาวคานารีรีสอร์ท อำเภอท่าใหม่ จังหวัดจันทบุรี, มีนาคม 2557, หน้า 397-401

ลิขสิทธิ์มหาวิทยาลัยเชียงใหม่
Copyright© by Chiang Mai University
All rights reserved



การถ่ายทอด พลังงานความร้อนและมวล

ในอุปกรณ์ด้านความร้อนและกระบวนการ ครั้งที่ 13

วันที่ 13-14 มีนาคม 2557

ณ เจ้าหลาว คาบาน่า รีสอร์ท จังหวัดจันทบุรี



Thermal Characteristics of Air Flow over Flat Tube with Ellipsoidal Dimpled Surface

Nopparat Katkhaw¹

Nat Vorayos¹

Atipoang Nuntaphan²

¹Department of Mechanical Engineering
Faculty of Engineering, Chiang Mai
University

Chiang Mai, Thailand, 50200.
Tel. 053-944146, Fax. 053-944145

Email: nopparat_ka@hotmail.com

Email: natvorayos@hotmail.com

²Thermal Technology Research Laboratory,
Mae Moh Training Center,
Electricity Generating Authority of Thailand,
Mae Moh, Lampang, Thailand 52220

Abstract In this study, heat transfer performance of the single-flat tube in cross flow was studied in comparison with bare-flat tube and tube bank was examined and the effect of tube space of single-row tube bank was also investigated. The stream air flows over the heated tubes and the velocity of air stream is varied from 1-3 m/s. The temperature and velocity of air stream, the temperature of tube surface and temperature of inlet and outlet tube bank were measured. The heat transfer of tube bank was determined. As the result, heat transfer enhancement is about 1.5 and 1.63 times for flat tube and flat-dimple tube respectively, compare to cylinder.

Keyword Vortex, Dimple, Enhanced Heat transfer

1. Introduction

The conventional enhanced heat transfer approaches; in general, involve the incorporation of fins, baffles, turbulizers and etc. to increase either the heat transfer surface area or turbulence or both. These approaches are effective in increasing heat transfer rates; hence, this also results to the significant pressure drops. Dimple indent is the configuration aiming at increasing heat transfer rates without significant sacrifice in pressure drop or fouling [1]. The dimpled plate and dimpled tubes give the superior to other approaches, as illustrated in Figure 1. Heat exchanger equipped with flat-finned tubes should give the higher heat transfer coefficient and less pressure drop than those with circular-finned tube. Applying the dimples on flat tube is possibly beneficial approach due to its potential in wake induction.

Recently, dimples or concave surfaces have been in focus extensively. In the early investigations, Afansayev et al. [2] investigated the overall heat transfer and pressure drop for turbulent flow of flat surface with staggered array of spherical dimples. Significant 30-40% increasing of heat transfer without significant pressure losses is reported. Chyu et al. [3] studied the heat transfer coefficient distributions of air flow in the channel over flat surface indent with staggered arrays of two different shapes of dimple. Their result shows the local heat transfer coefficients are significantly higher than values in the channels

with smooth surfaces. Enhancements of about 2.5 times of smooth surface values, and pressure losses are about half the values produced by conventional rib turbulators. Mahmood et al. [4] describe the flow structure above the dimpled flat surface. Flow visualizations showed vortical fluid as vortex pairs shed from the dimples. Their results showed the existence of a low heat transfer region in the upstream half of the dimple cavity followed by a high heat transfer region in the downstream half. Additional regions of high heat transfer were identified at the downstream rim of the dimple and on the flat surface of downstream of each dimple. Ligrani et al. [5] reported that as the H/D (Channel height to dimple diameter) increase the secondary flow structures and flow mixing intensified decreased. Nevertheless, Moon et al. [6] obtained almost a constant heat augmentation ratio of 2.1 for a dimpled passage with H/D from 0.37 to 1.49. Burgess et al. [7] reported that both the Nusselt number and the friction augmentation increased as the of dimple depth increased. Wang et al. [8] investigated a novel enhanced heat transfer tube with ellipsoidal dimples. Their computed results indicated that the Nusselt number for ellipsoidal dimpled tube and spherical dimpled tube are 38.6-175.1% and 34.1-158% higher than that for the smooth tube respectively. The friction factors of dimpled tube increase by 26.9-75% and 32.9-92% for ellipsoidal and spherical dimples compared with the smooth tube respectively. Katkhaw et al. [9] studied the heat

transfer of air flow over dimpled flat surface with the 14 types of dimpled arrangement. Their results show that heat transfer coefficient for dimpled surfaces are about 26% better than smooth surface for staggered arrangement. And for the inline arrangement, the results show that heat transfer coefficient for dimples surfaces are about 25% better than smooth surface.

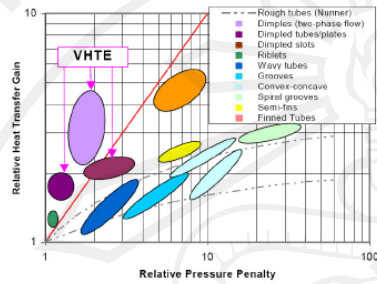


Figure 1 Compared to other types of heat transfer enhancement approaches. (From Chudnovsky and Kozlov [1])

In this work, flat-dimpled tube and tube bank without fins is in focus to study the heat transfer. Ellipsoidal dimple geometry will be used primarily.

2. Experimental setup and procedure

Figure 2 presents the schematic sketch of the experimental setup. In this experiment, the air stream generated by a centrifugal air blower was flowed over the heated plate with dimples. The velocity of air stream was controlled by the frequency inverter with the controllable range of 1-4 m/s. The velocity of air stream was measured by a hot wire anemometer with ± 0.2 m/s accuracy. The inlet temperature of air stream was measured by 4 sets of T-type thermocouple. The outlet temperature was measured by a T-type thermocouple mesh which consists of 16 thermocouples. Note that all of thermocouples have ± 0.1 °C accuracy. The surface temperature of flat tube was measured by infrared imaging camera with ± 2 °C accuracy. This temperature measuring instrument was also calibrated surface temperature with T-type thermocouple.

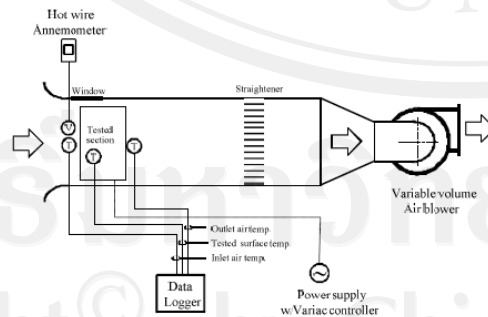


Figure 2 Schematic diagram of the experimental setup.

The tested section comprises three flat-dimpled tubes which made from steel. The 1500 watt of plate electric heater was plugged in the tube. The Iron powder was filled between the tube surface and plate heater to avoid air gap. Figs. 3 present the geometric details of the tested tube, including dimpled geometry. The S_T as shown in the figure is varied from 75 mm, 100 mm, and 125 mm.

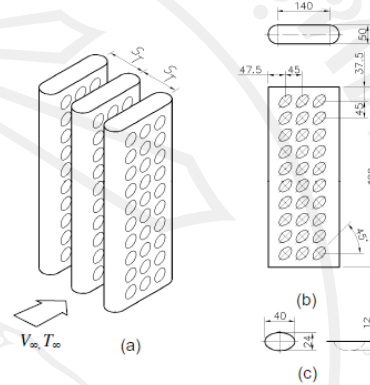


Figure 3 Details of: (a) dimpled-flat tube arrangement, (b) individual dimpled-flat tube geometry and (c) individual dimple geometry. All dimensions are in mm.

3. Data reduction

3.1 Single tube in cross flow

During the experiment, inlet air stream velocity, temperature, tube surface temperature and power supply were measured. The local heat transfer coefficient (h_x) is calculated from

$$h_x = q''_s / (T_s - T_\infty) \quad (3)$$

where q'' is surface heat flux. The heat flux is calculated from heat rate level at the tube under flat projected tube surface area. T_s is the local surface temperature and T_∞ is the temperature of inlet air stream flowing over the tested tube respectively.

The averaged air side heat transfer coefficient (h) of tested tube is determined by integrating all of the area of tube surface as

$$h = \frac{1}{A_s} \int_{A_s} q''_s / (T_s - T_\infty) dA_s \quad (4)$$

where A_s is tested surface area (flat projected tube surface area only).

The spanwise average Nusselt number (Nu_x) is defined as

$$Nu_x = \frac{h D_h}{k_f} \quad (5)$$

where $D_h = P/\pi$ and P is perimeter of tested tube, k_f is the thermal conductivity of air stream.

Reynolds number (Re_{Dh}) for air flow is defined as

$$Re_{Dh} = \frac{\rho_f V_f D_h}{\mu_f} \quad (6)$$

where ρ_f , V_f and μ_f are the density of air, the air frontal velocity and the dynamic viscosity of air stream respectively.

3.2 Tube bank in cross flow

During the experiment, inlet and outlet air stream velocity, temperature, the tube surface temperature and power supply were measured. The air side heat transfer rates can be calculated as

$$Q_a = \dot{m} C_p (T_{ao} - T_{ai}) \quad (7)$$

where Q_a is the heat transfer rate of air flow. For this studied, the average heat transfer rate is the mathematical average of the air side and the power supply of heater as

$$Q_{avg} = 0.5(Q_a + Q_e) \quad (8)$$

where Q_e is the electrical power supply.

The averaged air side heat transfer coefficient (h) of tested tube is determined by

$$h = Q_{avg} / (N A_s \Delta T_{lm}) \quad (9)$$

and ΔT_{lm} is a log-mean temperature difference which is defined as

$$\Delta T_{lm} = \frac{(T_{s,avg} - T_i) - (T_{s,avg} - T_o)}{\ln \left(\frac{T_{s,avg} - T_i}{T_{s,avg} - T_o} \right)} \quad (10)$$

where N is the total number of tubes in the bank, A_s is the surface area of one tube (flat projected surface area only), $T_{s,avg}$ is the average surface temperature, T_i and T_o air the inlet and outlet of air stream respectively.

The averaged Nusselt number (Nu_D) is defined as

$$Nu_D = \frac{hD}{k_f} \quad (11)$$

where D is tube width.

Reynolds number ($Re_{D,max}$) for air flow across tube bank is defined as

$$Re_{D,max} = \frac{\rho_f V_{max} D}{\mu_f} \quad (12)$$

where V_{max} is the maximum air velocity occurring within the tube bank.

This experiment is a further study from Katkhw et. al. [9]. The previous and current result will be in comparison with existing correlation of the heat transfer of parallel flow over flat plate with constant heat flux [10] under the laminar flow condition.

4. Results and discussion

4.1 Temperature distribution

The temperature distribution on the ellipsoidal dimpled tube surface was observed by using the infrared imaging

camera. The sample of result is shown in figure 4. As shown in the figure, the location of ellipsoidal dimples conforms to the ellipsoidal temperature contour. Whole area of plain surface is at lower temperature than dimple area. Higher temperature is located at the upstream halve and gradually increase along the downstream. The lowest temperature occurs in downstream rim of the dimples and obviously decreases along the downstream on plain surfaces. These results come from the recirculation of air stream in the dimpled.

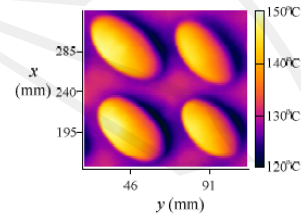


Figure 4 Temperature distributions along the plain surface of ellipsoidal dimple tube.

4.2 Single tube in cross flow

In this part, heat transfer of air flow across the flat tube and flat-dimple tube are studied. Figure 5 shows the variation of the local Nusselt number with surface length of cylinder, flat tube and flat-dimple tube in cross flow of air. Starting at the stagnation point, Nu_x of all tube configurations decreases with increasing surface distance as a result of laminar boundary layer development. For cylinder, a minimum is reached at angular dimension is about 80° and Nu_x increases with angular dimension due to vortex formation in the wake. On the other hand, Nu_x of flat tube and flat-dimple tube reach the minimum at surface distance is about 80 mm, which is on the plain surface. Both flat tube and flat-dimple tube have the same Nu_x trend line with the flat tube lagging by about 9%.

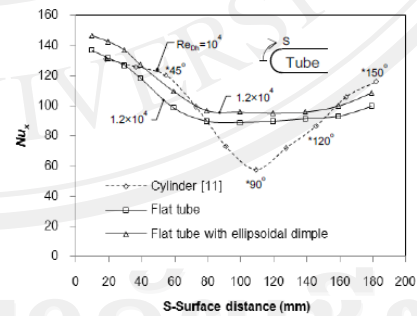


Figure 5 Average spanwise Nusselt number of cylinder, flat tube and flat-dimple tube. (*angular coordinate for cylinder)

Figure 6 shows the average air side heat transfer performance of cylinder, flat tube and flat-dimple tube. As shown

in the figure, flat tube and flat-dimple tube give the higher heat transfer coefficient than cylinder in same D_h and at all frontal velocities. Over a range of frontal velocity, enhancement of the average heat transfer coefficient is about 1.5 and 1.63 times for flat tube and flat-dimple tube respectively, compare to cylinder.

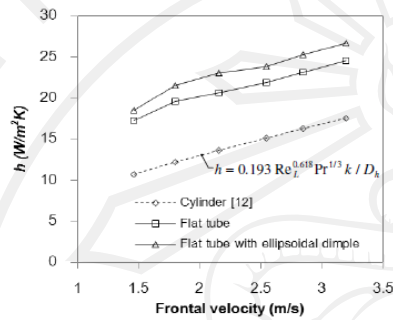


Figure 6 Average heat transfer coefficient for cylinder, flat tube and flat-dimple tube.

4.3 Tube bank in cross flow

In this part, heat transfer of air flow across single row tube bank is investigated. Tube bank comprises of three flat-dimple tube. The tube pitch (S_T/D) is varied from 1.5, 2 and 2.5. Figure 7 shows the effect of S_T/D to the air side heat transfer performance. As seen in the figure, Average heat transfer coefficient decrease as S_T/D increase due to the maximum air velocity passing the tube bank is increased with decreasing of tube pitch.

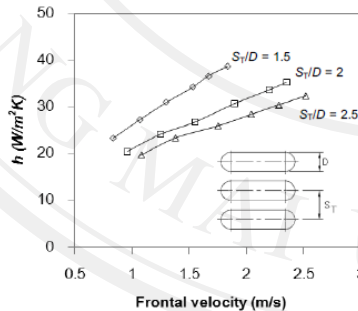


Figure 7 Average heat transfer coefficient to frontal velocity for tube bank.

4.4 Empirical Correlation

From the previous results, the multiple linear regression technique is performed to obtain the relevant correlation. The corresponding correlation is given as follows:

$$Nu_D = 0.1983 Re_{D,\max}^{0.618} Pr^{1/3} \quad (13)$$

Figure 8 shows the comparison of Nu of the experimental results with the proposed correlation. For the Nusselt number correlation Eq. (13) can predicts 95.1% and of the experimental data with $\pm 5\%$. The standard deviation of the correlation Eq. (12) is 1.8%.

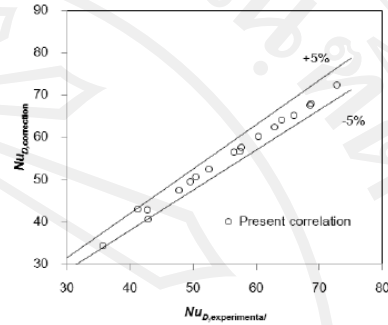


Figure 8 Comparison of Nu correlations with experimental data.

5. Summary and conclusion

The present study reports the heat transfer performance of air flow over the flat tube, flat-dimple tube and flat-dimple tube bank. The effect of tube pitch is examined. On the basis of previous discussions, the conclusions are made:

1. Air side heat transfer performance of flat tube and flat-dimple tube is augmented at all frontal velocity. The heat augmentation is approximately 60%.
2. Heat transfer enhancement is about 1.5 and 1.63 times for flat tube and flat-dimple tube respectively, compare to cylinder in the same surface area condition.
3. Correlation of the present experiment is developed. The proposed correlation yields fairly good predictive ability against the present test data.

Acknowledgement

The authors would like to thank the Thermal Technology Research Laboratory at Mae Moh Training Center Electricity Generating Authority of Thailand for facilitating the testing equipment and the Department of Mechanical Engineering, Faculty of Engineering, Chiang Mai University for funding this research study.

Reference

- [1] Y. Chudnovsky, A. Kozlov, Development and field trial of dimpled-tube technology for chemical industry process heaters, Final report, Industrial Technology Program, U.S. Department of Energy, September 2006.
- [2] V.N. Afanasyev, Y.P. Chudnovsky, A.I. Leontiev, P.S. Roganov, Turbulent flow friction and heat transfer characteristics

for spherical cavities on a flat plate. *Experimental Thermal and Fluid Science* 7 (1) (1993) 1-8.

[3] M.K. Chyu, Y. Yu, H. Ding, J.P. Downs, F.O. Soechting, Concavity enhanced heat transfer in an internal cooling passage, ASME Paper 97-GT-437, 1997

[4] G.I. Mahmood, M.L. Hill, D.L. Nelson, P.M. Ligrani, H.K. Moon, B. Glezer, Local heat transfer and flow structure on and above a dimpled surface in a channel, *Journal of Turbomachinery* 123 (1) (2001) 115-123.

[5] P.M. Ligrani, J.L. Harrison, G.I. Mahmood, M.L. Hill, Flow structure due to dimple depressions on a channel surface, *Physics of Fluids* 13 (11) (2001) 3442-3451.

[6] H.K. Moon, T. O'Connell, B. Glezer, Channel Height effect on heat transfer and friction in a dimpled passage, *Journal of Engineering for Gas Turbines and Power* 122 (2) (2000) 307-313.

[7] N.K. Burgess, P.M. Ligrani, Effects of dimple depth on channel Nusselt numbers and friction factors, *Journal of Heat Transfer* 127 (1) (2005) 839-847.

[8] Y. Wang, Y.L. He, Y.G. Lei, J. Zhang, Heat transfer and hydrodynamics analysis of a novel dimpled tube, *Experimental Thermal and Fluid Science* 34 (8) (2010) 1273-1281.

[9] N. Katkhaw, N. Vorayos, T. Kiatsiriroat, Y. Khunatorn, D. Bunturat, A. Nuntaphan, Heat transfer behavior of flat plate having spherical dimpled surfaces, *Journal of Mechanical Science and Technology*, Submitted.

[10] F.P. Incropera, D.P. Dewitt, T.L. Bergman, A.L. Lavine, *Introduction to Heat Transfer*, 5th ed., John Wiley & Sons, Asia, 2007.

[11] S. Kakac, R. K. Shah, W. Aung, *Handbook of single-phase convective heat transfer*, Wiley, New York, 1987

[12] R. Hilpert, *Forsh. Geb. Ingenieurwes*, 215 (4) (1993)

Nomenclature

A	Area (m^2)
D	Tube width (mm)
D_h	Hydraulic diameter (mm)
H	Wind tunnel height
Nu_t	Spanwise average Nusselt number base on tube width
Nu_D	Average Nusselt number base on tube width
Nu_0	Baseline average Nusselt number of flat tube without dimple
Pr	Prandtl number
Re_D	Reynolds number base on tube width
Re_{Dh}	Reynolds number base on hydraulic diameter
h	Average heat transfer coefficient ($\text{W}/\text{m}^2\text{K}$)
h_0	Average heat transfer coefficient of flat tube without dimple ($\text{W}/\text{m}^2\text{K}$)
h_x	Local heat transfer coefficient ($\text{W}/\text{m}^2\text{K}$)
T	Temperature ($^{\circ}\text{C}$)
V	Velocity (m/s)

CURRICULUM VITAE

Name Mr. Nopparat Katkhaw

Date of Birth April 2, 1977

Place of Birth Muang Sukhothai

Education 2007 M.Eng. in Mechanical Engineering,
Chulalongkorn University, 2007
2000 B.Eng. in Mechanical Engineering,
Chiang Mai University, 2000

Publications Nopparat Katkhaw, Nat Vorayos, Tanongkiat Kiatsiriroat,
Yottana Khunatorn and Damorn Bunturat, Atipoang
Nuntaphan, 2014. Heat Transfer Behavior of Flat Plate having
45° Ellipsoidal Dimpled Surfaces, *Case Studies in Thermal
Engineering*, 2, 67-74
Nopparat Katkhaw, Nat Vorayos, Atipoang Nuntaphan, 2014.
Heat Transfer Behavior of Flat Plate having Dimple Surfaces,
โครงการจัดประชุมวิชาการ การถ่ายเทพลังงาน ความร้อน และมวลใน
อุปกรณ์ด้านความร้อนและกระบวนการ ครั้งที่ 13, เจ้าหลวงคานานารี
สอร์ท อำเภอท่าใหม่ จังหวัดจันทบุรี, มีนาคม 2557
Nopparat Katkhaw, Nat Vorayos, Atipoang Nuntaphan, 2014.
Thermal Characteristics of Air Flow over Flat Tube with
Ellipsoidal Dimpled Surface, โครงการจัดประชุมวิชาการ การถ่ายเท
พลังงาน ความร้อน และมวลในอุปกรณ์ด้านความร้อนและกระบวนการ
ครั้งที่ 13, เจ้าหลวงคานานารีสอร์ท อำเภอท่าใหม่ จังหวัดจันทบุรี, มีนาคม
2557

